SOCIETY OF PETROLEUM ENGINEERS OF AIME
6200 North Central Expressway
Dallas, Texas 75206

PAPER NUMBER SPE 3474

THIS IS A PREPRINT --- SUBJECT TO CORRECTION

Analysis and Prediction of Gas Well Performance

By
K. H. Coats and J. R. Dempsey, Members AIME, International Computer Applications;
K. L. Ancell and D. E. Gibbs, Members AIME, Panhandle Eastern Pipe Line Company

This paper was prepared for the 46th Annual Fall Meeting of the Society of Petroleum Engineers of AIME, to be held in New Orleans, La., Oct. 3-6, 1971. Permission to copy is restricted to an abstract of not more than 300 words. Illustrations may not be copied. The abstract should contain conspicuous acknowledgment of where and by whom the paper is presented. Publication elsewhere after publication in the JOURNAL OF PETROLEUM TECHNOLOGY or the SOCIETY OF PETROLEUM ENGINEERS JOURNAL is usually granted upon request to the Editor of the appropriate journal provided agreement to give proper credit is made.

Discussion of this paper is invited. Three copies of any discussion should be sent to the Society of Petroleum Engineers office. Such discussion may be presented at the above meeting and, with the paper, may be considered for publication in one of the two SPE magazines.

ABSTRACT

This paper describes a numerical model for analyzing gas-well tests and predicting long-term deliverability. Field applications presented include an interpretation of a gas well test in a tight sand leading to an accurate long-term deliverability projection. The model presented numerically simulates two-dimensional (r-z) gas flow and accounts for effects of turbulence, skin, afterflow, partial penetration, pressure-dependent permeability and any degree of crossflow ranging from complete to none. Through a novel treatment of the equations describing reservoir flow, skin and afterflow, the model simulates shutin at the wellhead and then calculates afterflow and any subsequent circulation of gas through the wellbore from some layers to others.

References and illustrations at end of paper.

INTRODUCTION

Many gas wells exhibit pressure test behavior which is difficult if not impossible to interpret using conventional methods of analysis. Difficulty of interpretation is frequently encountered in low permeability reservoirs and in layered reservoirs with limited or incomplete crossflow. In these cases, assumptions in conventional analysis methods, such as complete (or no) crossflow and negligible effects of afterflow or interlayer recirculation through the wellbore, are frequently invalid.

This paper describes a numerical model which accounts for many factors which are neglected in conventional methods of analysis. The model numerically simulates two-dimensional (r-z), transient gas flow in a cylinder representing the drainage volume of a single well. The calculations account for effects of turbulence, skin, afterflow, partial penetration, pressure-dependent permeability and any degree of crossflow ranging from complete to none.

Equations describing gas flow in the reservoir, skin effect and afterflow are combined in a manner which allows simulation of shutin at wellhead rather than bottomhole; the model calculates afterflow and any recirculation of gas through the wellbore from some layers to others. Thus, the calculated results show the effects of afterflow and recirculation on shape of the pressure buildup curve.

Field applications presented illustrate use of the model to predict the long-term flow characteristics of gas wells prior to connection to a pipeline. The wells selected for illustration have been tested with both short and long-term tests to indicate the reliability of the method. An additional field application shows use of the model to explain and reproduce long-term (up to 600 days) gas well buildups.

The method presented is equally applicable to simulation of oil well tests and performance and the slightly modified equations for that case are given in the Appendix.

BRIEF DESCRIPTION OF THE MODEL

Equations comprising the model are described in detail in the Appendix. Only a brief outline of the method is presented here. The basic equation of the model is eq. (1) describing transient, two-dimensional (r-z) gas flow in a cylindrical drainage volume*:

$$\frac{1}{r}\frac{\partial}{\partial r}\left(\frac{rk_h b_g}{\mu_g}\frac{\partial p}{\partial r}\right) + \frac{\partial}{\partial z}\left(k_v\frac{b_g}{\mu_g}\frac{\partial p}{\partial z}\right) - q_v = \frac{\partial(\phi b_g)}{\partial t} \qquad (1)$$

Horizontal and vertical permeabilities, k_h and k_v, are arbitrary functions of r and z and formation volume is

$$b_g = \frac{pT_s}{1000\ Zp_sT}\ \frac{\text{Mcf}}{\text{cu. ft.}} \qquad (2)$$

Equations (1) and (2) are combined, expressed in terms of a gas potential and written in finite-difference form for the grid illustrated in Fig. 1. The result of these steps is a set of NRxNZ difference equations in the NRxNZ unknowns $\Phi_{i,j}$, i=1,2...,NR and j=1,2,...,NZ. NR and NZ are the numbers of grid blocks in the horizontal and vertical directions, respectively.

The gas potential Φ is defined as

$$\Phi = \int^{p} \frac{f(p)p}{Z\mu}dp \qquad (3)$$

where f(p) is permeability at p divided by permeability at initial pressure. If permeability does not vary with pressure then f(p) is 1.0 and eq. (3) becomes identical with the real gas potential [1].

The difference equations contain an additional set of NZ unknowns, $q_1, q_2, \ldots, q_{NZ}$ representing the flow rate (Mcf/D) into the wellbore from each layer. NZ additional equations give the additional pressure drop due to skin effect as

$$\Phi_{i,j} - \Phi = S_j q_j \qquad j=1,2,\ldots,NZ \qquad (4)$$

where S_j is related to the skin factor for layer j as described in the Appendix. Φ is gas potential evaluated at wellbore (bottomhole) pressure. Eq. (4) introduces the additional unknown Φ so that we now have NRxNZ+NZ+1 unknowns but only NRxNZ+NZ equations.

The final equation describes afterflow or wellbore accumulation as

$$q_j + q_2 + \ldots + q_{NZ} = q + C\frac{d\Phi}{dt} \qquad (5)$$

where q is wellhead production rate and C is a function of Φ, well radius and depth as defined in the Appendix. Eq. (5) is simply a gas material balance written about the wellbore volume as a system. This equation allows the flows from the layers q_j to be positive, zero or negative and allows flow from the formation even if wellhead rate q is 0. For each layer j in which the well is not completed the corresponding equation of eqs. (4) is replaced by $q_j=0$.

The above equations form a system of NRxNZ+NZ+1 simultaneous, nonlinear equations in the same number of unknowns. The unknowns are numbered in a manner such that the equations form a basically pentadiagonal, band matrix of band width 2xNZ+1. Gaussian elimination is employed to solve the equations after linearization. This direct (noniterative) solution eliminates almost entirely the convergence difficulties encountered with iterative methods in severely heterogeneous cases. We have treated with no computational difficulties cases of layer thicknesses varying from many feet to a fraction of an inch (representing a horizontal fracture) with corresponding layer permeabilities ranging from .001 md to several darcies.

The direct solution just described yields values each time step for flow from each layer, bottomhole flowing pressure and pressure distribution throughout the drainage volume. The bottomhole pressure is converted to flowing wellhead pressure using the Cullender-Smith equation [2].

Required input data for the model as described above are z and μ_g as functions of pressure, porosity, k_h and k_v as functions of layer and radius, initial pressure, well completion interval and production rate q as a function of time. A slightly modified formulation described in the Appendix allows specification of bottomhole flowing pressure as a function of time rather than wellhead production rate. Wellhead production rate replaces Φ as an unknown in this case. Turbulence is simulated using transmissibilities which are functions of flow rate.

FIELD APPLICATION 1

The well selected for this example is a completion at 6,550 feet. The well was badly damaged at completion and the test shown here reflects the condition at that time. Reservoir parameters are shown in the tabulation below:

Thickness	10 ft.
Porosity	11%
Water Saturation	44%
Permeability to Gas	20 md
Reservoir Temperature	607°R
Gas Gravity	0.632
Casing	4-1/2"
Tubing	2"
Initial Pressure	2522 psia

The well was produced for three days at a rate of approximately 475 Mcf/D. The well was then shut in and the pressure buildup was monitored with a bottomhole pressure bomb. These pressures are shown on Fig. 2.

A skin factor of 175 yielded agreement between observed and calculated drawdown prior to shutin. The corresponding calculated buildup portion of the test is shown on Fig. 2.

The badly damaged condition, coupled with the large volume of the wellbore resulted in an extended period of "afterflow." This period extended at least until the end of the first day of buildup. The capability of the model to accurately account for this phenomenon is graphically depicted on Fig. 2.

The "straight line portion" of the buildup curve starts at approximately one day and extends to the end, or about 2.5 days. This part of the curve is shown in detail on the small insert in Fig. 2. This portion can be plotted as a function of dimensionless time and analyzed analytically; the result is a formation permeability-thickness product of approximately 200 md-ft.

The wellbore volume can be reduced by setting the tubing on a packer. This will result in a shortened afterflow period which would make an analytical evaluation more reliable. This is illustrated on Fig. 3 as Case I. The only difference between the base case and Case I is the reduced wellbore volume caused by setting the tubing on a packer.

Another method to reduce the afterflow period would be to remove the wellbore damage or "skin." This can be easily done with the simulator and the result is shown on Fig. 3 as Case II. The drawdown rate was left the same even though it is possible to produce a much larger rate with skin removed. The result is a nearly straight line with very little character.

In summary, the test shown here illustrates the ability to simulate the actual performance of a well in considerable detail. Analysis of data in this manner enables an engineer to account for all the factors affecting the pressures that he measures without having to wait for the wellbore effects to die out.

FIELD APPLICATION 2

This application illustrates the use of the simulator as a tool to predict the long-term deliverability from a low permeability reservoir. The tool is ideal for this application because it accounts rigorously for the nonlinearity in the gas flow equation which is necessary when large pressure gradients exist in the reservoir.

The available reservoir data are summarized in the table below. The test data were taken over a six-month period between the dates that the well was drilled and connected to a pipeline. The data consist of three shutin pressures and four flow tests. The shutin periods varied in duration from three days to several months.

Zone	1	2
h, ft.	9	11
Ø, %	8.8	9.7
S_w, %	.280	.21
k, md	.15	.30
Depth, ft.	8609	8620
Temperature, °R	642°	642°
Gas Gravity	.604	.604
Initial Pressure, psia	3290	3290

The well was initially perforated, stimulated, and tested. The stimulation was simulated with an increased permeability in the vicinity of the wellbore. The first pressure buildup of 2785 psia was observed after three days of shutin. The well was then shut in for about 45 days and no known pressures were taken. The well was then flowed for a single day, shut in seven days, and a pressure of 3090 psia was observed. A very short-term 4-point test was then taken and the well was shut in for about four months. At the end of this four-month period, a pressure of 3290 psia was observed. The pressure behavior of the well, both calculated and observed is shown on Fig. 4. The flow test data, because of the short duration, are not shown here but actually were considered. The match shown on Fig. 4 was considered adequate as the basis of an extended prediction.

A simulation run was made assuming production into a 600 psi pipeline. The results are shown as the "predicted" curve on Fig. 5. The well has produced for four years and the actual production is shown as the "actual" curve on Fig. 5. This prediction represents what would have been done had this tool been available several years ago. The prediction shown on Fig. 5 is very adequate for any planning or economic evaluation that would have been necessary very early in the life of the well.

FIELD APPLICATION 3

This application treats a gas well which exhibited prolonged periods of pressure buildup--one period in excess of 600 days. Conventional analysis assuming a single layer of radial flow failed to explain the behavior in that a permeability sufficiently low to give the extended buildup period would not allow flow at the observed rates. The purpose of the well pressure analysis was estimation of gas reserves and long-term deliverability.

Logs and core analyses from wells in the field indicate gross and net pays of about 200 feet and 100 feet, respectively. Net pay horizontal permeabilities range from .1 to 50 md and porosities range from .03 to .14. The exterior radius for the well treated here has been roughly estimated as 1000-1500 ft. Wellbore radius is 3 in., initial reservoir bottomhole pressure is 3765 psia and reservoir temperature is 173°F. The well is perforated over about 60 feet of section.

Fig. 6 shows rate data and observed bottomhole pressure versus time for extended pressure buildups beginning 28 and 47 months after initial production from the well.

A number of simulator runs were performed with little success for several layered configurations and radial permeability variations. The reservoir "picture" finally employed with success stemmed from the hypothesis that the well communicated with a number of thin permeable stringers which in turn were fed by severely limited crossflow from large sand volumes. The simplest such description is a two-layer model with the well completed in the high permeability layer 1 and with a thicker layer 2 having very small horizontal and vertical permeability.

The three parameters in this description are the ϕh products of both layers and the effective vertical permeability for interlayer flow. A gradient search method was programmed into the simulator to determine in one computer submittal the best values of these three parameters. The results were porosity thickness products of .848 and 5.86 feet for layers 1 and 2, respectively, and an effective vertical permeability of .00007 md for flow between the layers. Horizontal permeabilities of 35 and 1 md were used for the two layers.

Fig. 6 shows the agreement between calculated and observed pressure buildups for these parameter values.

DISCUSSION

We have encountered a number of gas wells exhibiting extended periods of pressure buildup similar to the well described in Application 3 above. In all these cases we have found necessary a layered description where one or more tight layers bleed through severely limited crossflow into one or more thinner, permeable layers which connect to the well. With one layer of small or zero horizontal permeability bleeding into another permeable layer connecting to the well, the model simulates the case of a fractured matrix reservoir. The permeable layer represents the fracture conductivity and capacity while the second layer represents the tight matrix essentially communicating only pointwise with the fractures.

In some cases of deep, abnormally pressured gas wells we have found a better match of observed decline curves through using the pressure-dependent permeability feature of the model.

Numerical models of the type described here offer the advantage of accounting for many factors possibly affecting well behavior. Conventional analysis techniques such as Carter[3] generally ignore factors such as significant radial permeability variation, intermediate levels of crossflow, extended afterflow, etc. Swift and Kiel[4] show the effect of non-Darcy flow on well behavior. However, their results neglect the effects of crossflow, afterflow and recirculation on the behavior of the drawdown-buildup data. Watenbarger and Ramey[6], et al [5] show the applicability of using the "real gas potential"[1] definition for potential in Darcy's equation. However, here again recirculation and crossflow were neglected. Millheim and Aichowicz[7] discuss the combination of a linear flow model with the radial flow model to account for fracture flow in tight gas sands. Adams, et al[8] discuss further the use of the "real gas potential" to analyze fractured gas systems.

A disadvantage of the numerical model as an analysis tool is the trial and error nature of the approach, compounded by a large number of variables or parameters requiring determination. To an extent this disadvantage is offset by the considerable educational value received in the trial and error matching effort. Every well history is essentially a "short course" in itself, revealing in the matching effort the single and combined effects of skin, turbulence, afterflow, crossflow, heterogeneity, etc. on well performance. Invariably, several types of description are relatively quickly found inadequate to explain observed behavior. Then generally four or fewer parameters are found to essentially control the agreement between calculated and observed behavior. Further, the process is fast and inexpensive. An engineer can work a problem of the type shown here in a single working day or less and at a cost of approximately one minute of Univac 1106 computer time. This is not any more expensive than the standard analytic methods used for years.

In order to make the most effective use of this capability, a change in test philosophy is needed. To utilize analytic methods of transient pressure analysis, it is advantageous to maintain as nearly constant test rates as possible. However, the capability of the simulator to handle multiple transients makes it advantageous to introduce widely varying pressures by testing at several different rates for shorter periods of time. To get full advantage of the capability, the flow periods should be interspersed with periods of pressure buildup. This technique will introduce many transients which will help define any reservoir heterogeneity better than a single flow rate.

Finally, good turnaround on a digital computer aids the trial and error matching procedure. This turnaround is generally easily obtained with the model described here because of its low storage and computing time requirements. A problem using eight radial increments (layers) requires less than five seconds of CDC 6600 time for 50 time steps. We have found virtually no sensitivity to the number of radial increments (NR) provided NR exceeds about eight.

REFERENCES

1. Ramey, H. J., Jr. and Crawford, P. B., "The Flow of Real Gases Through Porous Media," Transactions, SPE, Vol. 237, I-624, 1967.

2. Katz, et al, Handbook of Natural Gas Engineering, McGraw-Hill, 1959.

3. Carter, R. D., "Solution of Unsteady-State Radial Gas Flow," Transactions, SPE, Vol. 225, I-549, 1962.

4. Swift, G. W. and Kiel, O. G., "The Prediction of Gas-Well Performance Including the Effect of Non-Darcy Flow," Transactions, SPE, Vol. 225, I-791, 1962.

5. Al-Hussainy, R. and Ramey, H. J., Jr., "Application of Real Gas Flow Theory to Well Testing and Deliverability Forecasting," Transactions, SPE Vol. 237, I-637, 1966.

6. Wattenbarger, R. A. and Ramey, H. J. Jr., "Gas Well Testing with Turbulence, Damage and Wellbore Storage," Transactions, SPE, Vol. 243, I-877, 1968.

7. Millheim, K. K. and Aichowicz, L., "Testing and Analyzing Low-Permeability Fractured Gas Wells," Transactions, SPE, Vol. 243, I-193, 1968.

8. Adams, A. R., Ramey, H. J., Jr. and Burgess, R. J., "Gas Well Testing in a Fractured Carbonate Reservoir," Transactions, SPE, Vol. 243, I-1187, 1968.

APPENDIX

MATHEMATICAL MODEL DESCRIPTION

Substitution of b_g from eq. (2) into (1) gives

$$\frac{1}{r}\frac{\partial}{\partial r}\left(\alpha r k_h \frac{f(p)p}{Z\mu}\frac{\partial p}{\partial r}\right) + \frac{\partial}{\partial z}\left(\alpha k_v\, f(p)\frac{p}{Z\mu}\frac{\partial p}{\partial z}\right)$$

$$- q_v = \alpha\phi\frac{\partial(g(p)p/Z}{\partial t} \qquad (6)$$

where k and ϕ are permeability and porosity, respectively, at initial pressure and α is $T_s/1000\ p_s T$. Defining gas potential Φ as in eq. (3), we have

$$\frac{1}{r}\frac{\partial}{\partial r}\left(\alpha r k_h\frac{\partial\Phi}{\partial r}\right) + \frac{\partial}{\partial z}\left(\alpha k_v\frac{\partial\Phi}{\partial z}\right) - q_v$$

$$= \alpha\phi c'\frac{\partial\Phi}{\partial t} \qquad (7)$$

where c' is $d[g(p)p/Z]/d\Phi$, a single-valued function of Φ.

An implicit difference approximation to eq. (7) is

$$(\Delta_r T_r \Delta_r \Phi + \Delta_z T_z \Delta_z \Phi)_{i,j,n+1} - q_{i,j}$$

$$= \frac{(V_p c)_{i,j}}{\Delta t} \delta \Phi_{i,j} \tag{8}$$

Radial transmissibility for flow between r_{i-1} and r_i, (where $\{r_i\}$ are "block center" radii) are defined by

$$T_{ri-1/2,j} = \frac{\alpha 2\Pi \; \Delta z_j \; k_{hi-1/2,j}}{\ln r_i/r_{i-1}} \tag{9a}$$

where the effective interblock permeability $k_{hi-1/2,j}$ must be

$$k_{hi-1/2,j} = \frac{\ln r_i/r_{i-1}}{\int_{r_{i-1}}^{r_i} \frac{d \ln r}{k(r)}}$$

to correctly relate steady flow rate and pressure drop in the interval r_{i-1}, r_i for the case of a given permeability distribution k(r). Permeability is eq. (9a) is expressed as md x .00633.

Transmissibility for vertical flow between layers j-1 and j is defined by

$$T_{zi,j-1/2}$$

$$= \frac{\alpha\Pi(r^2_{mi+1/2} - r^2_{mi-1/2})k_{vi,j-1/2}}{.5(\Delta z_j + \Delta z_{j-1})} \tag{9b}$$

where the effective interblock permeability must be

$$k_{vi,j-1/2} = \frac{.5(\Delta z_j + \Delta z_{j-1})}{\int_{z_{j-1}}^{z_j} \frac{dz}{k_v(z)}},$$

$r_{mi+1/2}$ is the log mean radius $(r_{i+1} - r_i)/\ln(r_{i+1}/r_i)$ and z_j is the depth to the center of layer j.

The accumulation or capacity coefficient,

$$(V_p c)_{i,j} = \alpha\Pi(r^2_{mi+1/2} - r^2_{mi-1/2})$$

$$\phi_{i,j} \frac{(g(p)\frac{p}{Z})_{i,j,n+1} - (g(p)\frac{p}{Z})_{i,j,n}}{\Phi_{i,j,n+1} - \Phi_{i,j,n}} \tag{10}$$

is a chord slope (with respect to Φ) of the term representing gas-in-place in the grid block. The term $r_{mi-1/2}$ for i=1 is $r_1=r_w$. The sink term $q_{i,j}$ is the production rate from grid block i,j, Mcf/D. Each term in eq. (8) has units of Mcf/D.

Difference notation is

$$\Delta_r T_r \Delta_r \Phi_{i,j,n+1}$$

$$= T_{ri+1/2,j}(\Phi_{i+1,j} - \Phi_{i,j})_{n+1}$$

$$- T_{ri-1/2,j}(\Phi_{i,j} - \Phi_{i-1,j})_{n+1}$$

$$\Delta_z T_z \Delta_z \Phi_{i,j,n+1}$$

$$= T_{zi,j+1/2}(\Phi_{i,j+1} - \Phi_{i,j})_{n+1}$$

$$- T_{zi,j-1/2}(\Phi_{i,j} - \Phi_{i,j-1})_{n+1}$$

$$\delta\Phi = \Phi_{i,j,n+1} - \Phi_{i,j,n}$$

For clarity of presentation, our remaining discussion will be pertinent to a system of eight radial grid blocks extending from specified r_w to r_e and four layers. The term $q_{i,j}$ is zero everywhere except for blocks at i=1 (at the well). We number the grid blocks and variables $\Phi_{i,j}$ linearly starting with 1 at i=NR, j=1, 2 at i=NR, j=2, etc., proceeding down first and then in toward the well. Thus the linear index m is

$$m = (NR-i) \times NZ + j \tag{11}$$

and the eq. (8) can be written in terms of m as

$$a_{m,m-NZ}\Phi_{m-NZ} + a_{m,m-1}\Phi_{m-1}$$

$$- a_{m,m}\Phi_m + a_{m,m+1}\Phi_{m+1}$$

$$+ a_{m,m+NZ}\Phi_{m+NZ} - q_m = b_m \tag{12}$$

where b_m is $-(V_pc)_{i,j}\ \Phi_{i,j,n}/\Delta t$ and the off-diagonal a coefficients are transmissibilities. Eq. (12) written for m=1,2,...,32 is a system of 32 equations in the 36 unknowns $\{\Phi_m, m=1,32\}$ and $\{q_m, m=29,30,31,32\}$. The terms q_m (m=29-32) are the flow rates into the wellbore from the four layers. The transmissibilities $T_{ri-1/2,j}$ must be set to 0 for i=1 in eq.(8) since these q terms account for flow into the well. Also, $T_{rNR+1/2,j}$ for j=1,2,...,NZ are zero representing the closed exterior boundary and the closed boundaries at z=0 and z=H are represented by $T_{zi,j-1/2} = 0$ for j=1, NZ+1.

The additional potential drop at the wellbore surface in each layer due to skin is

$$\Phi_{i,j} - \Phi = \frac{1}{2\Pi\Delta z_j\ k_{hj}}\ \text{SKIN}(j)\ q_{i,j}$$

or in terms of m,

$$\Phi_m - \Phi = s_m q_m \qquad m = 29,30,31,32 \tag{13}$$

where k_{hj} is layer j permeability at the well at initial pressure and Φ is the value of $\int^p f(p)\frac{p}{Z\mu}\,dp$ at p = bottom-hole wellbore pressure. If the well is not completed in a given layer then the corresponding equation of the set (13) is simply replaced by $q_m = 0$.

Counting the four equations (13), we now have 36 equations in the 37 unknowns $\{\Phi_m\}$, $\{q_m$, m=29-32$\}$ and Φ. The final equation accounts for after-flow and is simply a mass balance on the wellbore gas-filled volume. A static well pressure gradient is assumed in integrating the static head equation to obtain

$$G_{wb} = \frac{144\ \Pi r_w^2\ T_s R}{1000\ Mp_s}(p_{bh} - p_{wh})$$

$$G_{wb} = C\ p_{bh} \tag{14}$$

where

$$C = \frac{144\ \Pi r_w^2\ T_s R}{1000\ Mp_s}\left(1-e^{-\frac{MD}{144\ Z_a RT_{wa}}}\right)$$

The mass balance on the wellbore is

$$q_{29} + q_{30} + q_{31} + q_{32} = q + \frac{\delta G}{\Delta t}$$

or

$$q_{29} + q_{30} + q_{31} + q_{32}$$

$$= q + C_{\prime}\delta\Phi = q + C_{\prime}(\Phi - \Phi_n) \tag{15}$$

where

$$C_{\prime} \cong C\frac{p_{bhn+1} - p_{bhn}}{\Phi_{n+1} - \Phi_n} \tag{16}$$

and q is specified wellhead production rate.

Eqs. (12), (13) and (15) are 37 equations in the above mentioned 37 unknowns. The equations form a band matrix of band width 2xNZ+1. The q_m terms are counted as unknowns 33, 34, 35, 36 and $\Phi(\equiv\Phi_{n+1})$ is number 37.

If flowing bottomhole pressure p_{bh} is specified rather than q then the equations above are unchanged except that q is now unknown 37 taking the place of (known) Φ.

The 37 equations (12), (13) and (15) are solved directly by Gaussian elimination. The chord slope coefficients eqs. (10) and (16)) can be approximated at the beginning of each time step by the slopes at $\Phi_{i,j,n}$ as determined from tables of the functions $g(p)p/z$ and p versus Φ. For large pressure (potential) changes over the time step 2 or 3 "outer" iterations can be performed where the chord slopes are re-evaluated and the 37 equations resolved. We have found on the great majority of problems that no iteration is necessary --i.e. the answer is not significantly changed by iterating.

The above equations apply with minor changes to the case of single-phase oil flow. The potential for the oil case is defined as

$$\Phi = \int^{p} \frac{f(p)\ b_o(p)\ dp}{\mu_o} \qquad (17)$$

and the right-hand side (capacity) coefficient involves the chord slope of the function $g(p)\ b_o(p)$ with respect to Φ. The coefficient C in the counterpart to eq. (14) relating wellbore oil volume to bottomhole pressure can be easily derived for the two cases of a freely flowing or pumped well.

In the case of turbulent flow Darcy's law is modified to [2]

$$-\frac{dp}{dr} = \frac{\mu}{k} v + \beta \frac{Mp}{ZRT} v^2 \qquad (18)$$

for radial flow. Integrating this equation for a constant flow q Mcf/D from r_i to r_2 yields

$$q = T_{rt}(\Phi_1 - \Phi_2) \qquad (19)$$

where subscript t denotes modification of the transmissibility due to turbulence,

$$T_{rt} = \frac{\alpha' k_h}{\ln\frac{r_2}{r_1} + \frac{\beta M k_h}{\alpha' RT\mu} q\left(\frac{1}{r_1} - \frac{1}{r_2}\right)} \qquad (20)$$

and

$$\alpha' = 2\Pi\alpha\Delta z$$

At the beginning of each time step the transmissibility T_{rt} can be evaluated using in the denominator the value of q existing at the end of the previous time step. We found a more stable and satisfactory procedure is to expand eq. (19) as a quadratic in q, use the value of $\Phi_1 - \Phi_2$ existing at the beginning of the time step (time n) to calculate q and use that q to evaluate T_{rt}. Of course T_{rt} can be updated using iterations similar to the chord slope treatment. We have found iteration on the q term in T_{rt} to be unnecessary.

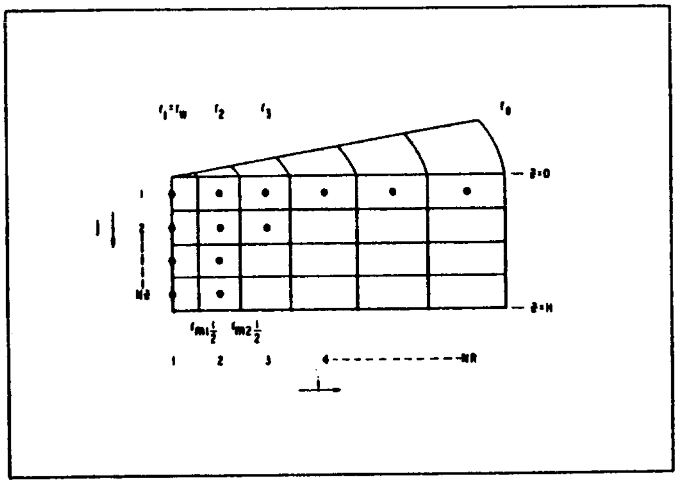

Fig. 1 - Schematic of the Physical System

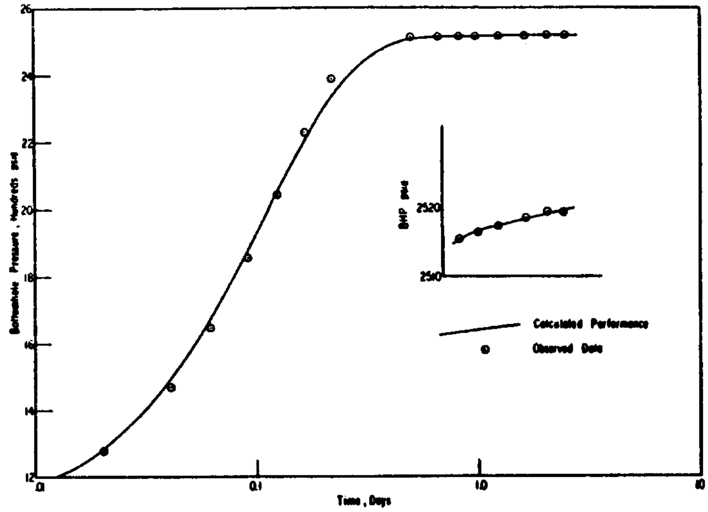

Fig. 2 - Field Application #1 Pressure Buildup Test

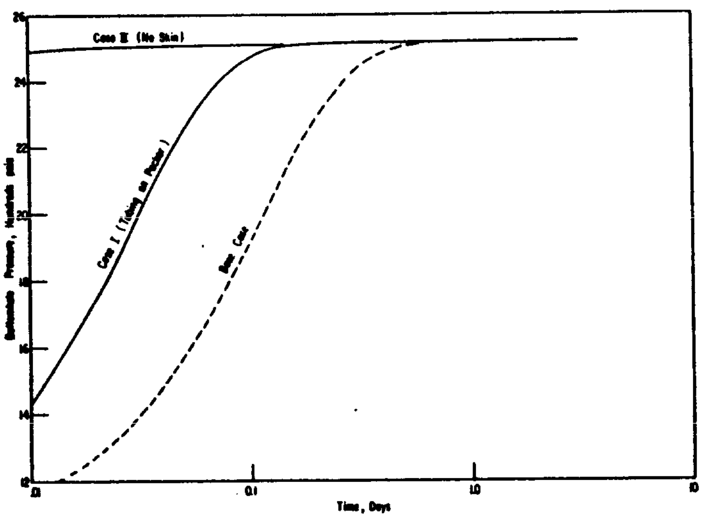

Fig. 3 - Field Application #1 Analysis of Completion

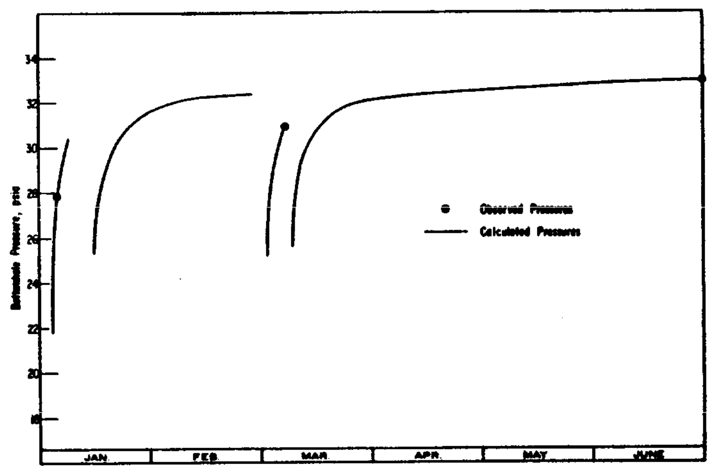

Fig. 4 - Field Application #2 Test Analysis

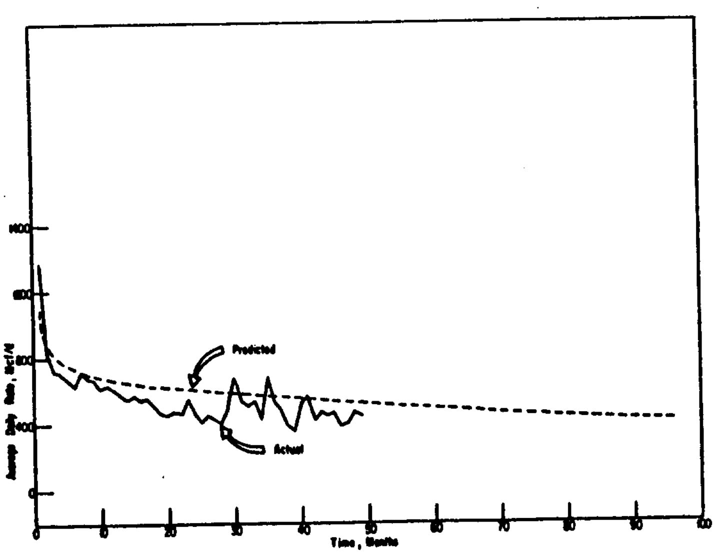

Fig. 5 - Field Application #2 Predicted and Actual Production

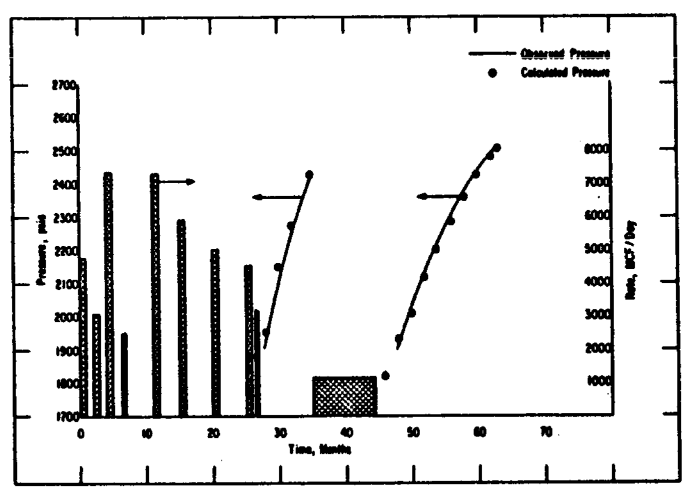

Fig. 6 - Field Application #3 Comparison of Observed vs. Calculated Pressure